Contents lists available at ScienceDirect

# Construction and Building Materials

journal homepage: www.elsevier.com/locate/conbuildmat

# ASR induced by chloride- and formate-based deicers in concrete with non-reactive aggregates

A. Antolik [*], D. Jóźwiak-Niedźwiedzka

*Institute of Fundamental Technological Research Polish Academy of Sciences, Pawiński 5b, 02-106 Warsaw, Poland*

A B S T R A C T

Despite ongoing efforts to prevent the damaging effects of alkali-silica reaction (ASR) in concrete structures, this phenomenon still exists and causes significant degradation. This study aims to investigate the role of various deicing agents in provoking ASR by examining volume expansion, cracks, and microstructure of mortar and concrete containing aggregates identified as non-reactive by standard ASR test methods. To achieve this, the concrete specimens undergo simulated operating conditions testing to induce ASR expansion, with an external supply of alkali from chloride- and formate-based deicers. The findings suggest that the configuration and concentration of the deicing agent used, as well as the mineral composition of the aggregate that was previously identified as non-reactive, can significantly impact the expansion and damage caused by ASR. The results indicate that existing methods for testing aggregates for ASR may have limitations when formate-based agents are used.

## 1. Introduction

Alkali-silica reaction (ASR) is a common problem in civil engineering structures that can cause significant deterioration of concrete. For this deleterious reaction to occur, three conditions must be met: reactive aggregate (containing reactive silica), high pH in the pore solution (alkali hydroxides $Na^+$, $K^+$ and $OH^-$), and high humidity (>80% relative humidity). If these conditions are met, an expansive silica-rich gel can form, leading to concrete expansion and cracking [1–3].

Despite efforts to prevent and mitigate the effects of alkali-silica reaction on concrete structures, there is still an increasing number of areas experiencing significant deterioration. Over the last few years, ASR has been widely found in hydropower plants and bridges [1,4–10], but this damaging reaction has also been observed on concrete roads and airport pavements [11–15]. In all these cases, reactive aggregates were used. Even concrete mixtures with low-alkali cements have suffered deleterious ASR [15]. The above examples refer mostly to concrete roads and airport pavements, i.e., places where deicing chemicals are applied. Deicing agents are an additional source of alkali and dissolve calcium hydroxide, which increases the pH of the pore solution due to the increase in the concentration of $OH^-$ ions; these factors can trigger ASR [16–18]. Deicing agents containing sodium, potassium, and calcium can penetrate the concrete and react with the silica in the aggregate, leading

to expansion and cracking [15,16,19]. Moisture and high temperatures can further accelerate this reaction [20–23]. The use of deicing agents, such as potassium or sodium formate, is considered to be more environmentally friendly than chloride-based deicing agents, but they can still have impact on ASR [15]. Moreover, deicing agents can increase moisture in the concrete by melting snow and ice, exacerbating the ASR reaction. [24].

Chloride-based deicers may have detrimental effects on concrete infrastructure – often resulting in expansion, mass change, reduced dynamic modulus of elasticity, [25] and most of all, reduced strength, [26]. Past studies [27–32] on the effects of chloride based deicers on concrete vary greatly, depending on factors such as exposure conditions, deicer concentrations, and test temperature. Additionally, the research on the impact of deicers on concrete durability has mainly focused on the chemical degradation of cement paste [27,33–35]. To assess accelerating effect of deicers on ASR, relatively low temperature test conditions (below or equal to 38 °C) were used for a limited duration, up to one month [35–37]. The research performed by Desai [33] was focused on the effects of chloride deicers on alkali silica reactivity, but apart from the variations in exposure conditions and cement type, the aggregate was limited only to sand fractions, while the coarse aggregate was not taken into consideration. Rajabipour et al. [16] stated that the NaCl ingress into concrete, as a deicing salt, has been thought to

exacerbate certain cases and laboratory studies of ASR, while having no effect on expansion in others. The conclusion from the study by Yicheng [34] was that under certain exposure conditions the deicers with alkali ions (i.e. NaCl) may increase the potential for ASR in systems with reactive aggregate whereas the effect of the other deicers is more related to the chemical attack on the components of the hydrated paste.

Deicing of airport pavements requires the use of alternative deicing agents due to the harmful effects of chlorides on aircraft – sodium and potassium formates or acetates are used. However, like NaCl, they can serve as an additional source of alkali that accelerates ASR. In the past decade, interest in the effect of potassium acetate on alkali-silica reaction in reactive aggregate has grown [15–18,30,38]. The research conducted by Giebson et al. [15] revealed that deleterious ASR can be initiated and accelerated in concretes with reactive aggregates exposed to deicers, especially acetates and formates, even with low-alkali cement. Contrary conclusions were drawn by Wang et al. [30], they didn't found drastic damage on macro and micro scale or presence of ASR products, despite using a high concentration of potassium acetate (54.4 wt%). Positive effect of supplementary cementitious materials like fly ash or slag on reducing ASR-induced expansion have been reported [17,39]. Julio-Betancourt [38], analysing the effect of potassium acetate on ASR, noticed a positive effect of its dilution, resulting in much lower concrete damage. However, discrepancy between laboratory and field tests should be noted. Hayman et al. [17] found significant damage to concrete treated with potassium acetate in the laboratory tests, however they didn't observe it in field specimens after 3 years of research.

It was found that the external supply of chloride-based deicers as well as acetates and formates and pre-existing microcracks had a significant impact on ASR-induced deterioration of highway and airport pavement concrete containing alkali-reactive aggregates [27,40,41]. However, deicing agents can play a major role in causing an ASR reaction in aggregates considered non-reactive by standard ASR test methods. The constant access of alkalis from deicing agents can increase the concrete mixture's alkali content and accelerate the ASR [42,43]. The effect of deicing agents on inducing or accelerating the alkali-silica reaction in aggregates identified as non-reactive by standard ASR test methods is still not fully recognized.

Igneous rocks are formed through the cooling and solidification of molten magma or lava. Intrusive igneous rocks, also known as plutonic rocks, are created when magma cools and solidifies beneath the Earth's surface. Due to slow cooling, intrusive rocks have a coarse-grained texture, allowing for the growth of large mineral crystals. [44]. Aggregates produced from intrusive igneous rocks are considered high-quality concrete aggregate, known for their strength and resistance to environmental impacts. Gabbro, granodiorite and granite rocks are commonly considered to be ASR non-reactive by standard ASR test methods [45], however they may contain reactive forms of quartz like micro- and cryptocrystalline quartz or strained quartz [46]. Recently, the topic of reactivity of aggregates from intrusive igneous rocks, especially granites, has been discussed more frequently [12,47–49]. Strained quartz is a slowly reactive mineral component of aggregates, this is why the degradation of concrete structure may appear later [49,50]. Even without external alkali access, in the concrete used at the Three Gorges Dam in China, it has been shown that granite aggregate can release alkalis into the concrete, which can contribute to ASR [51].

The objective of the study was to evaluate the effect of chloride and formate-based deicers on the alkali-silica reactivity of aggregates identified as non-reactive by standard ASR test methods in concrete pavements. The microstructure of concrete was analysed under simulated conditions with added deicers as an external alkali source. The research highlights that the impact of deicers on ASR in concrete with aggregates identified as non-reactive by the standard ASR test methods depends on various factors such as the type and quantity of the deicer used and the concrete's exposure conditions.

## 2. Materials and methods

### 2.1. Materials

Three aggregates from intrusive igneous rocks were selected to test the influence of deicing agents on the potential of alkali silica reaction: granite aggregate (G), granodiorite aggregate (GD), and gabbro aggregate (GA). The deposits of aggregates were located in southern Poland. The selection of aggregates was based on their widespread use in construction of road and airport pavements resulting from the high quality of the rocks [52]. Aggregates of 2–8, 8–16 and 16–22 mm fractions were tested. The chemical composition of the tested aggregates, obtained by X-ray fluorescence (XRF) and their physical properties are presented in Tables 1 and 2, respectively.

Two Portland cements were used for mortar bars and concrete prisms preparation. The chemical composition of cements used was presented in Table 3.

### 2.2. Methods

#### 2.2.1. Mineral and chemical composition

Petrographic analysis of the aggregate was performed according to Polish Technical Guidelines [54] to analyse presence of reactive minerals. Thin sections ($25 \times 40$ mm, $30 \pm 2$ μm thickness) were prepared for each aggregate and the detailed description of the procedure is presented in [12]. Observations in transmitted light with crossed polarized plates (XPL) and plane polarized plates (PPL) were conducted using an Olympus BX51 polarizing microscope equipped with a digital colour camera.

Chemical composition analysis of aggregates and cements (Tables 1 and 3) was carried out using a Wavelength Dispersive X-ray Fluorescence Spectrometer (WD-XRF) Philips PW 2400. Test was performed on powdered specimens (grain size below 63 μm).

#### 2.2.2. Alkali-silica reactivity

Accelerated mortar-bar test (AMBT) and long-term concrete-prism test (CPT) were used to induce alkali-silica reactivity of aggregates from intrusive igneous rocks.

AMBT was performed in accordance with RILEM AAR-2 [55] standard. Mortar bars ($25 \times 25 \times 285$ mm) were made of Portland cement CEM I 52,5 R with a high alkali concentration ($Na_2O_{eq} = 0.87\%$) and water to cement ratio 0.47. The AMBT test was modified to evaluate the effect of three different deicing agents on the ASR. Standard 1 M NaOH solution, for storage of specimens at 80 °C, was replaced with the deicing agent solutions: 50% of potassium formate (HCOOK), 15% of sodium formate (HCOONa) or 10% of sodium chloride (NaCl), each separately. The concentrations of the deicing agents solutions were selected to reflect the real winter deicing conditions. The potassium formate is used at a concentration of 50% by weight, not only when ice is present, but also preventively on non-ice surface. The sodium formate is primarily used in its solid state. However, in our research, we specifically focused

**Table 1**
X-ray fluorescence chemical composition of tested aggregates, % wt.

| Compound | G [%] | GD [%] | GA [%] |
|---|---|---|---|
| $SiO_2$ | 73.07 | 56.87 | 46.59 |
| $TiO_2$ | 0.26 | 0.89 | 0.86 |
| $Al_2O_3$ | 14.22 | 13.65 | 13.49 |
| $Fe_2O_3$ | 2.02 | 7.86 | 10.44 |
| MnO | 0.05 | 0.14 | 0.16 |
| MgO | 0.4 | 5.72 | 10.81 |
| CaO | 1.81 | 6.76 | 10.89 |
| $Na_2O$ | 3.76 | 2.50 | 2.44 |
| $K_2O$ | 3.8 | 3.58 | 0.15 |
| $P_2O_5$ | 0.07 | 0.96 | 0.14 |
| $(SO_3)$ | <0.01 | 0.1 | <0.01 |
| SUM | 99.82 | 99.53 | 99.51 |

**Table 2**

Basic physical properties of aggregates used in concrete pavements determined by standard procedures PN-EN 12620 [53].

| Properties | Standard | G | GD | GA |
|---|---|---|---|---|
| Volume density [mg/m$^3$] | PN-EN-1097-6:2002 [37] | 2.63 | 2.69 | 2.91 |
| Water absorption [%] | | 0.7 | 0.2 | 0.9 |
| Category of resistance to fragmentation | PN-EN-1097-2/2000 [38] | LA$_{40}$ | LA$_{25}$ | LA$_{15}$ |
| Frost resistance | EN-1367-1:2001 [39] | F1 | F1 | F1 |

on the concentration of 15%, as required by the NO-17-A205 [56] standard for deicing effectiveness testing.

CPT was performed in accordance with RILEM AAR-3 [57] standard. Concrete prisms (75 × 75x285 mm) were prepared with CEM I 52.5 R with a high alkali concentration of 0.87% of Na$_2$O$_{eq}$ (Table 3). To ensure the alkali content of 1.25% of the cement weight, sodium hydroxide was added to the mixing water. The test was carried out in the following variant: tested fine aggregate (0.125–4 mm) combined with non-reactive coarse aggregate (amphibolite aggregate of 4–22 mm fraction; expansion of mortar bars according to RILEM AAR-2 after 14 days was 0.036% < 0.050%).

ASR tests with deicing solutions were also performed under simulated operating conditions according to RILEM AAR-12 [58]. For specimens preparation (75 × 75 × 285 mm prisms) Portland cement CEM I 42,5 R with a low alkali content was used (Na$_2$O$_{eq}$ = 0.56%, Table 3). The mixture proportions and cement were selected in such a way as to be suitable for slip-formed pavement concrete exposed to XF4 aggressive environment. Properties of fresh and hardened concrete mixture are presented in Table 4. Crushed aggregate from igneous rocks was used as coarse aggregate with a maximum grain size of 16 mm (G) or 22 mm (GD, GA). Natural river quartz sand was used as fine aggregate (0–2 mm) and it constituted 30% of the total aggregate. The ASR reactivity of siliceous sand was tested according to RILEM AAR-2 and mortar bars with it reached expansion of 0,04% (<0.050%) after 14 days, classifying it as non-reactive. To ensure the frost resistance of concrete, it was air entrained using an admixture based on a synthetic surfactant in the amount of about 1.5% of the cement mass to obtain the target fresh air content of 5–7%. Additionally, 100 mm cubes were formed for compressive strength measurement (according to PN-EN 12390 [59]). After 28 days of pre-conditioning, concrete-prisms were measured: length, mass, modulus of elasticity (Grindosonic equipment). The specimens were then subjected to ten 14-day cycles, each consisting of: 6 days of drying at 60 °C, 2 days of storage in deicing agent solution, 6 days of storage in a thermostatic chamber at 60 °C and high humidity conditions (RH > 98%), 1 day of storage in sealed containers at 20 °C and high humidity conditions (RH > 98%). After each cycle, the specimens were measured again. The following were used as deicing agent solutions (the same as in the modified AMBT test): 10% NaCl, 15% HCOONa, 50% HCOOK and as a reference distilled water. For granite aggregate (G), tests were also performed in dilute solutions: 10% HCOONa and 25% HCOOK.

### 2.2.3. Microstructure

Specimens treated with deicing agents, mortar-bars (AAR-2) and concrete-prisms (AAR-12) were cut and prepared for microstructure observations using a scanning electron microscope (SEM). Post-mortem specimens were cut (25 × 40 × 10 mm), dried for 3 days at 50 °C and impregnated with epoxy resin. Then, the specimens were grinded on

diamond discs (125, 75, 54, 18 and 9 μm) and polished using diamond pastes (6, 3, 1 and 0.25 μm). After surface preparation, the specimens were dried again for 3 days at 50 °C and sputtered with carbon (about 20 nm). Microstructure observations were performed on a JEOL JSM-6460LV microscope equipped with an energy-dispersive X-ray spectral analysis (EDS) detector (PV72-55050 EDAX, AMETEK, USA, Genesis Spectrum 6.2 software by EDAX Inc.). The SEM was operated with acceleration voltage set to 20 kV, an aperture 120 μm and working distance of 10 mm.

EDS analysis of the chemical composition of the ASR gel was performed in the form of atomic ratio Ca/Si and (Na + K)/Si. The gel found in the cracks of the aggregate and in the air voids was analysed. About 200 point determinations of the chemical composition were made for each specimen.

## 3. Results

Different types of aggregates from igneous rocks were characterized by varying silica content, Table 1. Granite aggregate contained the highest amount of silica (73.05%), then - granodiorite aggregate (56.87%) and the least in gabbro aggregate (46.59%). The alkali content in the aggregates was presented in the same order: G (Na$_2$O – 3.76%, K$_2$O – 3.8%), GD (Na$_2$O – 2.50%, K$_2$O – 3.58%), GA (Na$_2$O – 2.44%, K$_2$O – 0.15%). Significant differences were noted in the presence of Fe$_2$O$_3$, MgO and CaO: gabbro aggregate contained the highest amount, granodiorite aggregate less and granite aggregate the least.

Petrographic analysis was carried out to identify reactive silica in the tested aggregates. The images obtained in cross (XPL) and plane-polarized light (PPL) are presented in Figs. 1–3. Microcrystalline quartz and strained quartz were found in all aggregates, however, the presence of microcrystalline quartz was traceable. The surface content of strained quartz in the aggregates was calculated based on the methodology presented in [12]. Granite aggregate contained 1.8% of strained quartz, granodiorite aggregate – 2.7% and gabbro aggregate had 0.2%. The content of reactive ingredients in all aggregates was low enough to not induce ASR.

The results of the aggregate ASR potential reactivity, performed according to standard methods, are shown in Fig. 4. Elongation of mortar bars after 14-day exposure in 1 M NaOH solution at 80 °C showed that expansion was below the limit of 0.1% for all aggregates (0.054% – G, 0.059% – GD and 0.017% – GA). Expansion of concrete prisms during 365-day exposure at 38 °C confirmed the AMBT results and showed a similar trend, with expansion below the limit of 0.04% for all aggregates

**Table 4**

Composition and properties of concrete mix., according to RILEM AAR-12 requirements [58].

| Constituents | G | GD | GA |
|---|---|---|---|
| Cement CEM I 42.5 [kg/m$^3$] | 360 | 360 | 360 |
| Coarse aggregate | granite 2–16 mm | granodiorite 2–22 mm | gabbro 2–22 mm |
| Fine aggregate, 0–2 mm | river quartz sand | river quartz sand | river quartz sand |
| w/c | 0.45 | 0.45 | 0.45 |
| Slump [mm] | 100 | 60 | 70 |
| Fresh air content [%] | 0.8 | 0.8 | 0.7 |
| Compressive strength, f$_{c28}$ [MPa] | 49.4 ± 2.1 | 48.4 ± 3.4 | 50.6 ± 2.9 |

**Table 3**

X-ray fluorescence chemical composition of Portland cement used, % wt.

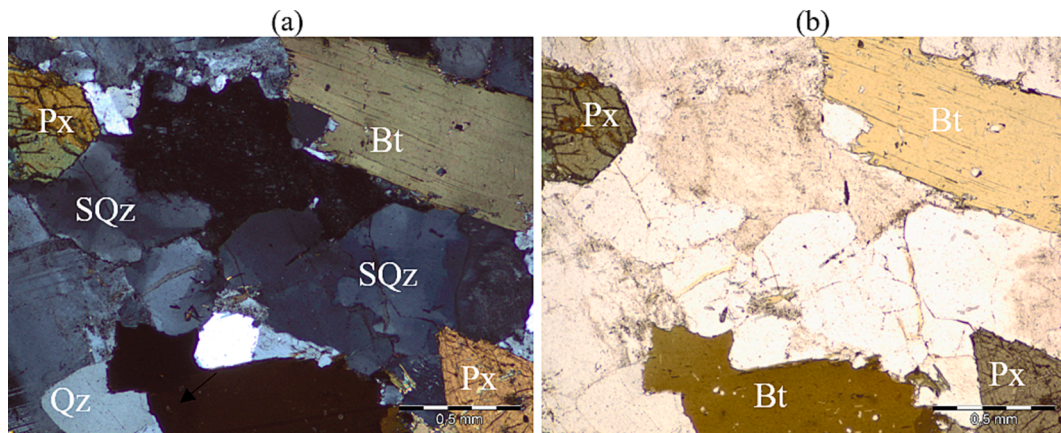| Cement | SiO$_2$ | Al$_2$O$_3$ | Fe$_2$O$_3$ | CaO | MgO | SO$_3$ | Na$_2$O | K$_2$O | Na$_2$O$_{eq}$ | LOI |
|---|---|---|---|---|---|---|---|---|---|---|
| CEM I 42.5 R | 19.03 | 4.84 | 3.22 | 63.64 | 1.15 | 2.97 | 0.21 | 0.53 | 0.56 | 3.34 |
| CEM I 52.5 R | 19.42 | 5.15 | 2.94 | 64.10 | 1.75 | 3.50 | 0.29 | 0.88 | 0.87 | 2.43 |

**Fig. 1.** The microphotographs of the analysed granite aggregate (G) in a) XPL and b) PPL, Qz – quartz, SQz – strained quartz, Bt – biotite, Px – pyroxene.
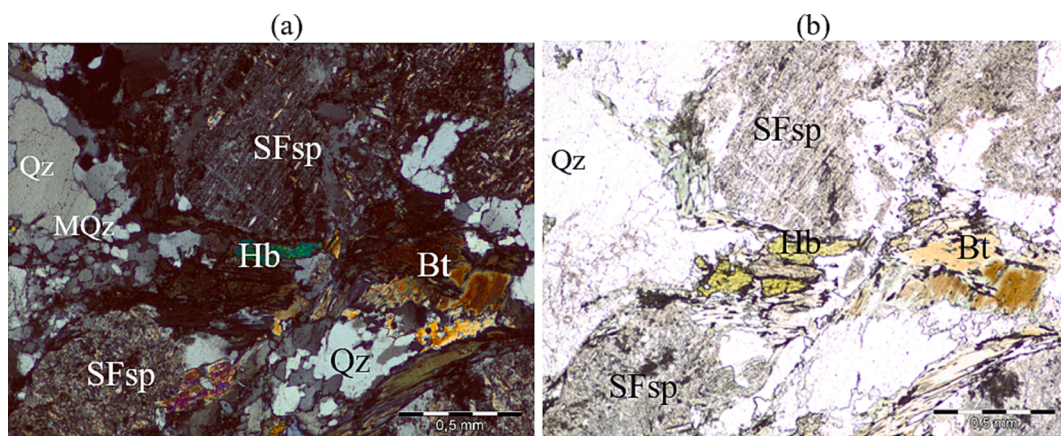


**Fig. 2.** The microphotographs of the analysed granodiorite aggregate (GD) in a) XPL and b) PPL, Qz – quartz, MQz – microcrystalline quartz, SFsp – feldspar alteration to sericite, Bt – biotite, Hb – hornblende.
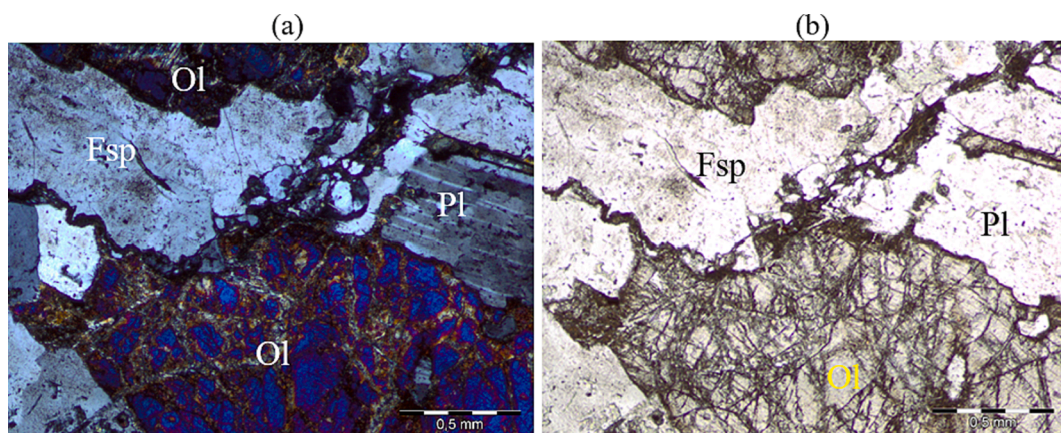


**Fig. 3.** The microphotographs of the analysed gabbro aggregate (GA) in a) XPL and b) PPL, Ol – olivine, Fsp – feldspar, Pl – plagioclase.

(0.036% – G, 0.034% – GD, 0.023 – GA). However, in concrete with granite and granodiorite aggregate, the expansion was close to the limit. Based on the above results, the aggregates were classified as non-reactive.

The results of the AMBT test, modified with different deicing salts solutions, are presented in Fig. 5. The scale of the vertical axis in the figures varies due to the different impact of the deicing agents. The influence of the 10% NaCl and 15% HCOONa solution on mortar-bars expansion at 80 °C was negligible, with elongation of the mortar bars

at around 0.01% after 28 days, while the use of 50% HCOOK resulted in much higher expansion: 0.645% – G, 0.997% – GD, 0.159% – GA. Also, the differences between the expansion of mortars with different aggregates became visible. Mortar-bars with gabbro aggregate showed 6 times less expansion than mortars with granodiorite aggregate (which had the largest expansion).

The expansion of concrete prisms with three aggregates from igneous rocks during the test under simulated operating conditions was presented in Fig. 6. The expansion of concrete prisms and the decrease in
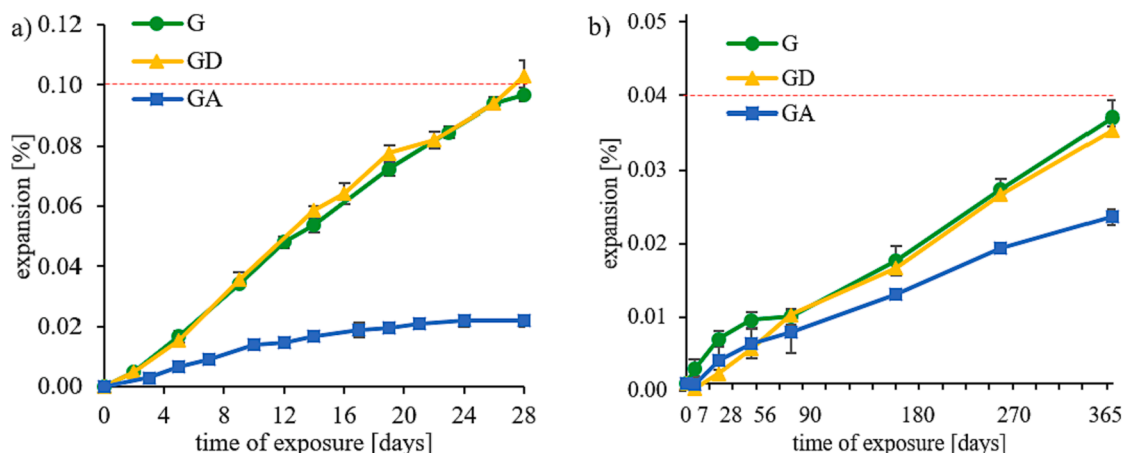
**Fig. 4.** Expansion of (a) mortar bars with different aggregates from igneous rocks during 28-day exposure in 1 M NaOH solution in 80 °C (AMBT), (b) concrete prisms with different aggregates from igneous rocks during 365-day exposure in 38 °C and high humidity conditions (CPT).

elastic modulus after 10 cycles of the test were presented in Tables 5 and 6, respectively. Specimens that were stored in distilled water during test cycles showed the lowest expansion (0.23–0.32 mm/m) and decrease in elastic modulus (from 3.60 to 1.12%). Introducing a solution which is not chemically aggressive, was aimed to check what degree of destruction is the result of physical interactions: cyclical changes in temperature and humidity. A clear influence of the type of deicing agent on the expansion and decrease in the modulus of elasticity of concrete prisms tested under simulated operating conditions was observed. The highest expansion (2.10–5.00 mm/m) and decrease in the modulus of elasticity (from 34.42 to 41.38%) were found for concrete specimens stored in a 50% HCOOK solution. Minor damage was caused by a 15% HCOONa solution (expansion 1.22 to 1.67 mm/m, a decrease in the modulus of elasticity from 8.15 to 15.84%) and a 10% NaCl solution (expansion from 0.33 to 0.70 mm/m, decrease in the modulus of elasticity from 4.53 to 8.10%). In the RILEM AAR-12 test, the limit of expansion for 10% NaCl solution is 0.5 mm/m. The limit has been exceeded by the concrete prisms with granite and granodiorite aggregate. Expansion of concrete prisms with gabbro aggregate was much smaller.

Reducing the concentration of the sodium formate solution by a third and two-fold reduction in the concentration of the potassium formate solution did not cause a proportional decrease in the expansion of concrete specimens. A larger difference was observed with the use of a less aggressive agent – 10% sodium formate – which resulted in a reduction of expansion by 31% in comparison to 15% HCOONa. The use of 25% HCOOK resulted in a reduction of 13% expansion compared to 50% HCOOK solution.

In microscopic analysis, an abundance of ASR products was found in concrete specimens after testing under simulated operating conditions using various deicing agents solution. ASR gel was identified in all specimens exposed to deicing agents solutions: 10% NaCl, 15% HCOONa and 50% HCOOK. No ASR products were found in specimens stored in distilled water. Across the specimen cross-section, micro-cracks (about 1–5 μm) in the cement matrix and a few cracks in the coarse and fine aggregate grains were observed. In specimens stored in deicing agents solutions numerous macro- and micro-cracks were observed in the cement matrix over the entire cross-section of specimen regardless of the type of deicing salt. ASR gel the most often was found in aggregate cracks (Figs. 7–9). ASR products were also found in the interfacial transition zone (Fig. 12) and in the air voids.

In specimens stored in 50% HCOOK, aggregate grains partially or completely reacted into ASR gel, as shown in Fig. 10. Quantitative analysis of the gel content in the specimens was difficult to perform, but a much higher amount of ASR products was found in concrete specimens after storage in 50% HCOOK than in the specimens stored in other deicing agents solutions. Also, the presence of a new phase (probably

tricarboaluminate, $3CaO \cdot Al_2O_3 \cdot 3CaCO_3 \cdot 32H_2O$) in the air voids was identified in the specimens stored in the formate-based solutions (50% HCOOK and 15% HCOONa) as shown in Fig. 11.

In Table 7, the chemical composition of alkali-silica reaction products localized in cracked aggregate grains cracks in concrete after testing under simulated operating conditions is presented (RILEM AAR-12). The type of deicing agent had the greatest impact on the chemical composition of the ASR gel. The same origin aggregate from the igneous rocks were used in the tests, therefore the type of aggregate did not have a significant influence on the chemical composition of the ASR gel. The largest differences in the ASR gel were found in the amount and type of alkali. In specimens tested in 10% NaCl solution, (Na + K)/Si was 0.21–0.31 and Na/K was 1.48–1.91. ASR gel found in specimens tested in 15% HCOONa contained slightly more alkali (Na + K)/Si: 0.34–0.36, and a higher sodium to potassium ratio (Na/K: 1.63–2.03) compared to specimens tested in sodium chloride. The highest content of alkali (Na + K)/Si: 0.51–0.62, was found in the gel in specimens tested in 50% HCOOK, additionaly no sodium ions were found, while potassium accounted for 100% of alkali.

In the mortar specimens after the modified RILEM AAR-2 test with deicing agents both crystalline and amorphous ASR products were found. In the SEM images, the gel in a crystalline form was identified by its characteristic rosette-like structure, as shown in Fig. 13. Depending on the ASR gel form, differences in the chemical composition were observed. The amorphous ASR gel contained more calcium and slightly less alkali (Ca/Si = 0.65, Na + K/Si = 0.38) than the crystalline (Ca/Si = 0.41, Na + K/Si = 0.46) ASR gel. In the analysed materials, amorphous gel was dominant.

## 4. Disscusion

The conducted research shows that, that even aggregates identified as non-reactive by the standard ASR test methods can be susceptible to ASR in a chemically aggressive environment. Standard ASR testing methods focus on identifying the reactivity of aggregates in the presence of alkali hydroxides. The sensitivity of such methods in evaluating the reactivity of aggregates in the presence of deicing and anti-icing agents is not fully known. In countries where ASR is a serious problem, the impact of de-icing agents on concrete pavements has begun to be considered but mainly for chloride-based salts [60,61,58]. Since the introduction of saturated NaCl bath method in Denmark for sand analysis, no new structure has developed alkali–silica reaction and distress [62]. Since 2013, new requirements for concrete road pavements have been introduced in Germany to reliably prevent damage to ASR road surfaces [61]. Based on the German method [61], the assumptions of the RILEM method were adopted to test the resistance of concrete
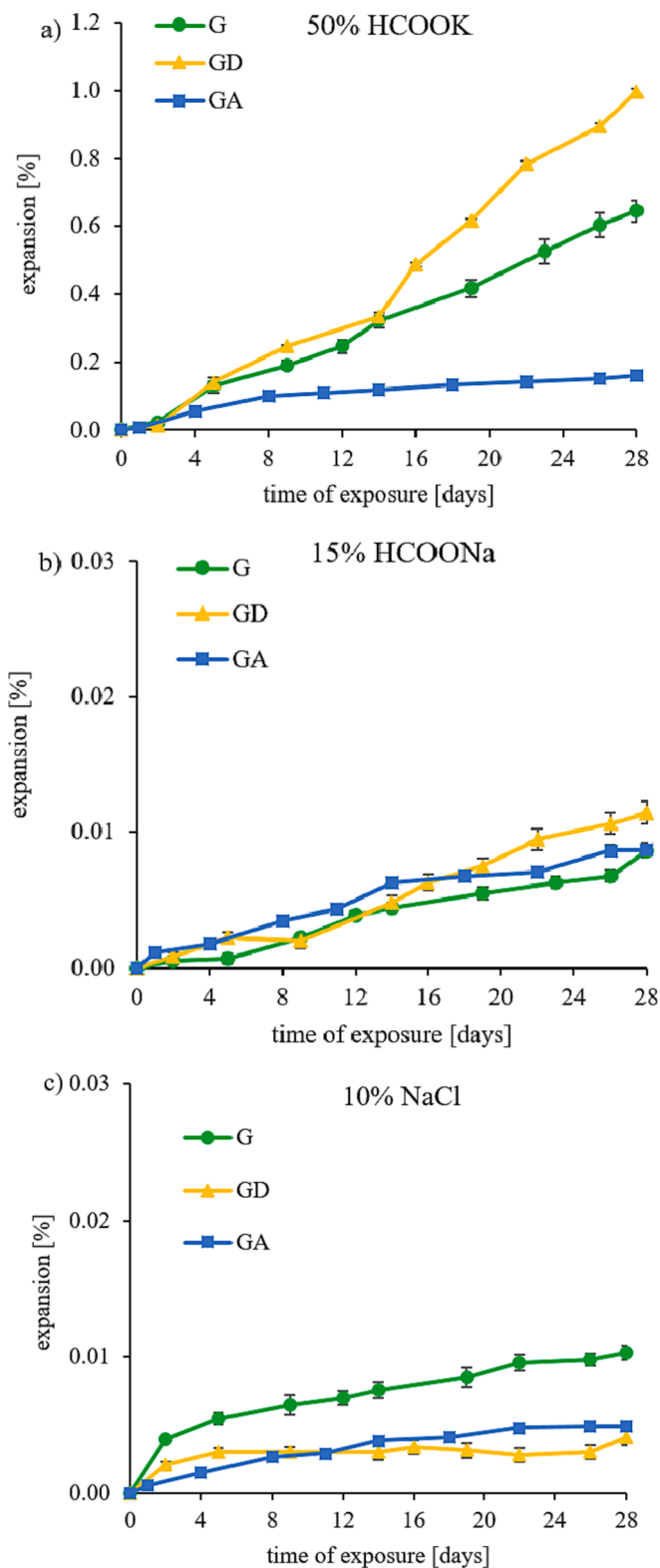
**Fig. 5.** Expansion of mortar bars with different aggregates from igneous rocks during 28-day exposure in (a) 50% HCOOK, (b) 15% HCOONa, (c) 10% NaCl solution.

compositions to alkali-silica reactivity with external alkali supply [58]. Preliminary study on the improvement of a research method for identifying the reactivity of aggregates in the presence of potassium acetate was proposed by Math el al. [62]. They found that the sensitivity of an aggregate to undergo alkali-silica reactivity in the presence of potassium

acetate deicer can be ascertained using the proposed revised EB-70 test method.

In presented results all aggregates were classified as non-reactive, based on the AAR-2 and AAR-3 method, however the presence of reactive minerals has been found. Micro- and cryptocrystalline quartz was present only in trace amount, strained quartz was in a greater amount. Despite the relatively low content of reactive components in all aggregates, a very high expansion was achieved in a test under simulated operating conditions, according to RILEM AAR-12. Expansion limit (0.5 mm/m) for test with 10% NaCl solution has been exceeded for specimens with granite and granodiorite aggregate. Expansion of concrete with gabbro aggregate was well below the limit. These results are consistent with the rest of the research: RILEM AAR-2, RILEM AAR-3 and petrography, specimens with gabbro aggregate was characterized by the lowest expansion and content of reactive minerals. The use of formate-based deicing agents has not been described in RILEM AAR-12 method therefore there is no standard expansion limit for the use of sodium and potassium formate. However, it can be noticed that the expansion of concrete prisms exposed to HCOOK or HCOONa is much higher than NaCl. Concrete with granite aggregate has reached more than two times greater expansion in 15% HCOONa (1.67 mm/m) and seven times greater expansion in 50% HCOOK (5.00 mm/m) than in 10% NaCl storage (0.70 mm/m). Concrete with granodiorite aggregate had more than three times greater expansion in 15% HCOONa (1.75 mm/m) and five times greater expansion in 50% HCOOK (5.00 mm/m) than in 10% NaCl storage (0.52 mm/m). Concrete prisms with gabbro aggregate also achieved high expansion in 15% HCOONa (1.22 mm/m) and in 50% HCOOK (2.10 mm/m). Deicing agents were not the only factor influencing the expansion of concrete specimens in this study: variability of humidity (wetting/drying) as well as temperature also play an important role in the destruction process. It is known from the literature that cyclic wetting and drying could cause concrete deterioration [63–65]. Drying results in removal of water from the air voids, leading to shrinkage and formation of micro-cracks. On the other hand, wetting, even though it allows water to be reabsorbed into the microstructure, does not ensure that the effects caused during the drying process will be completely reversed [63]. Cracks caused by cyclic wetting and drying accelerate the ingress of the deicer's ions [64]. Alkalis from de-icing agents penetrate deeper, resulting in ASR acceleration and greater expansion associated with ASR gel formation. On the basis of the conducted research, it was found that the use of formate-based deicers significantly accelerated the process of concrete destruction [16,66,67]. Concrete that was not exposed to de-icing agents (storage in distilled water), but only to wetting and drying cycles, had significantly lower expansion compared to concrete that was exposed to de-icing agents.

The influence of deicing agents was not so obvious in the case of the results obtained in modified AMBT method. Mortar bars exposed to 50% HCOOK solution achieved the highest expansion as well as concrete prisms in RILEM AAR-12 test. However, specimens stored in 15% HCOONa and 10% NaCl were characterized by a slight expansion (about 0.01% after 28 days). Applying modified AMBT test may not be an appropriate method to identify the effects of deicing agents on ASR in aggregate. In particular, specimens exposed to sodium formate showed contradictory results, for which very high expansion was obtained in the AAR-12 test and very low in the AAR-2 test.

In conducted research, the strong influence of organic salts deicers on the durability of concrete was showed, unlike Wang et al. [30], which didn't find the presence of ASR products or drastic damage of concrete, despite the use of a high concentration of potassium acetate. The harmful effect of potassium formate was found both in the AMBT method and in the cyclic method. Reduction of concentration of potassium formate in AAR-12 test from 50% to 25% did not result in a significant reduction in concrete expansion (reduction of only 13%) in contrast to Julio-Betancourt [38].

Ternary diagram of the chemical composition of the gel located in the cracks of the aggregate grains and in the air voids in concrete-prisms
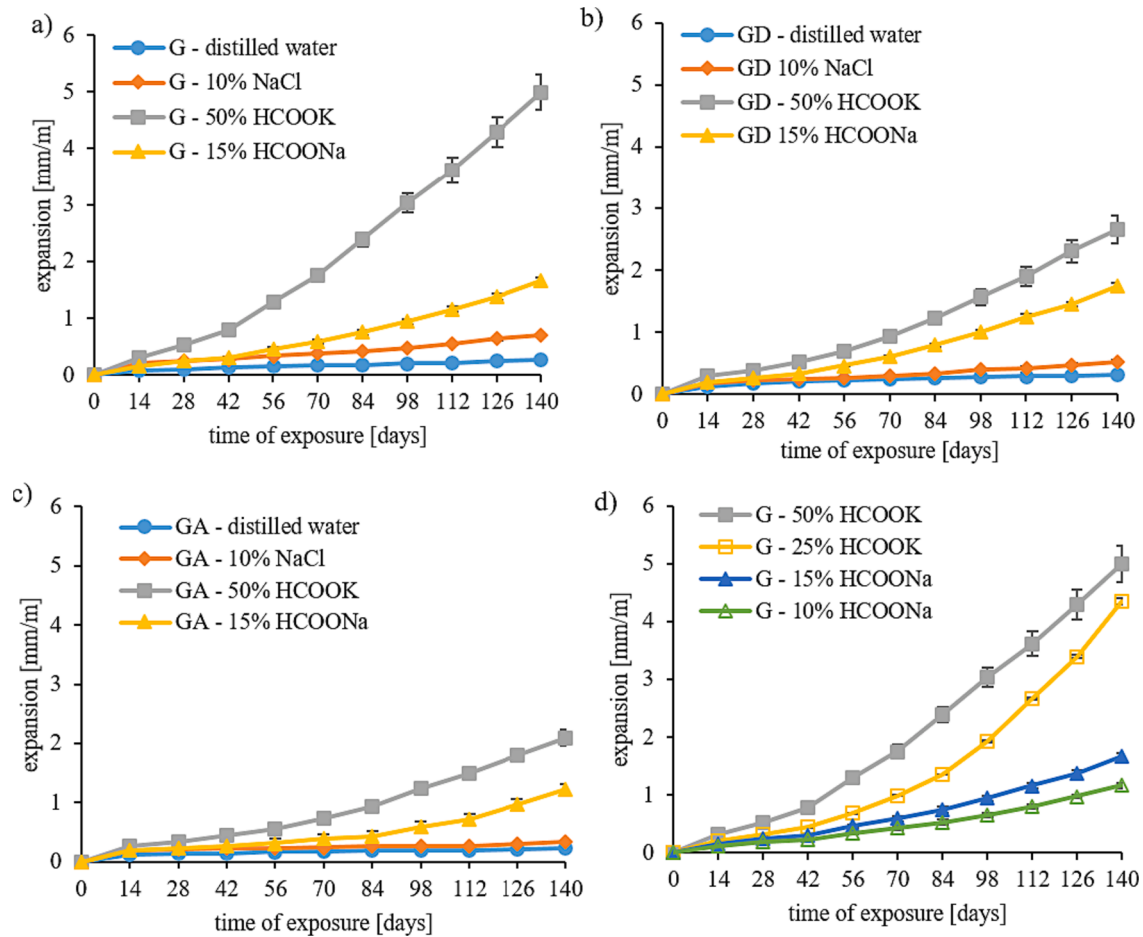
**Fig. 6.** Expansion of concrete prisms under simulated operating conditions (RILEM AAR-12) with the use of various deicing agents, (a) with granite aggregate, (b) with granodiorite aggregate, (c) with gabbro aggregate, (d) using different concentrations of sodium and potassium formate for concrete with granite aggregate.

**Table 5**

Expansion [mm/m] of concrete prisms subjected to simulated operating conditions (RILEM AAR-12) with the use of various deicing agents after 10 cycles.

| Aggregate | The solution used/deicing agent | | | |
|---|---|---|---|---|
| | Distilled water | 10% NaCl | 15% HCOONa | 50% HCOOK |
| G | 0.27 ± 0.01 | 0.70 ± 0.01 | 1.67 ± 0.05 | 5.00 ± 0.17 |
| GD | 0.32 ± 0.02 | 0.52 ± 0.02 | 1.75 ± 0.04 | 2.66 ± 0.15 |
| GA | 0.23 ± 0.01 | 0.33 ± 0.02 | 1.22 ± 0.06 | 2.10 ± 0.14 |

**Table 6**

Change of the elastic modulus [%] of concrete prisms subjected to simulated operating conditions (RILEM AAR-12) with the use of various deicing agents after 10 cycles.

| Aggregate | The solution used/deicing agent | | | |
|---|---|---|---|---|
| | Distilled water | 10% NaCl | 15% HCOONa | 50% HCOOK |
| G | −3.60 ± 0.03 | −8.10 ± 0.11 | −15.84 ± 0.11 | −41.38 ± 0.85 |
| GD | −1.54 ± 0.03 | −3.30 ± 0.11 | −15.72 ± 0.19 | −35.74 ± 1.49 |
| GA | −1.12 ± 0.02 | −4.53 ± 0.06 | −8.15 ± 0.21 | −34.42 ± 1.68 |

after testing in simulated operating conditions were presented in Fig. 14. The type of deicing agent used had the greatest influence on the chemical composition of the ASR gel. ASR products identified in the cracks in the aggregate in concrete, which was exposed to potassium formate, were characterized by the highest alkali content (triangle points shifted towards the Na + K vertex) while the lowest content of

alkali was found in specimens exposed to sodium chloride (square points). Changes in the content of calcium within the ASR gel located in the cracks in the aggregate were not clearly noticeable. The shift of the points towards a higher calcium content is visible in the ASR products identified in the air voids. Due to the selected type of aggregate intended for concrete pavements, only aggregates from intrusive igneous rocks were selected, therefore the chemical composition of ASR products formed was similar regardless of aggregate type. The variability of chemical composition of ASR products was showed by Leemann et al. [68] and Strack et al. [69], but they used more mineralogically diverse aggregates.

Chemical composition of ASR products has influence on its swelling properties [70]. The ASR gel identified in the cracks in aggregate grains was characterized by a similar calcium content, regardless of the deicing agent and aggregate used. Ca/Si value ranged from 0.26 to 0.45 and according to literature [71] ASR gel with this chemical composition has increased swelling capacity and water absorption. On the other hand, the ASR gel identified in air voids was characterized by an increased content of calcium (Ca/Si from 0.79 to 1.17), which implies that ASR gel had reduced expansion capacity [72]. It was supposed that ASR gel in air voids didn't show expansion, but its presence was still unfavorable due to frost resistance.

It was found that the type of deicing agent had a significat effect on the content and type (Na, K) of alkali in the ASR gel. The lowest alkali content was found in concrete exposed to sodium chloride (Na + K)/Si from 0.21 to 0.31, slightly more was observed in concrete exposed to sodium formate – from 0.34 to 0.36, while the highest in concrete exposed to potassium formate – from 0.51 to 0.62. In [71] was shown
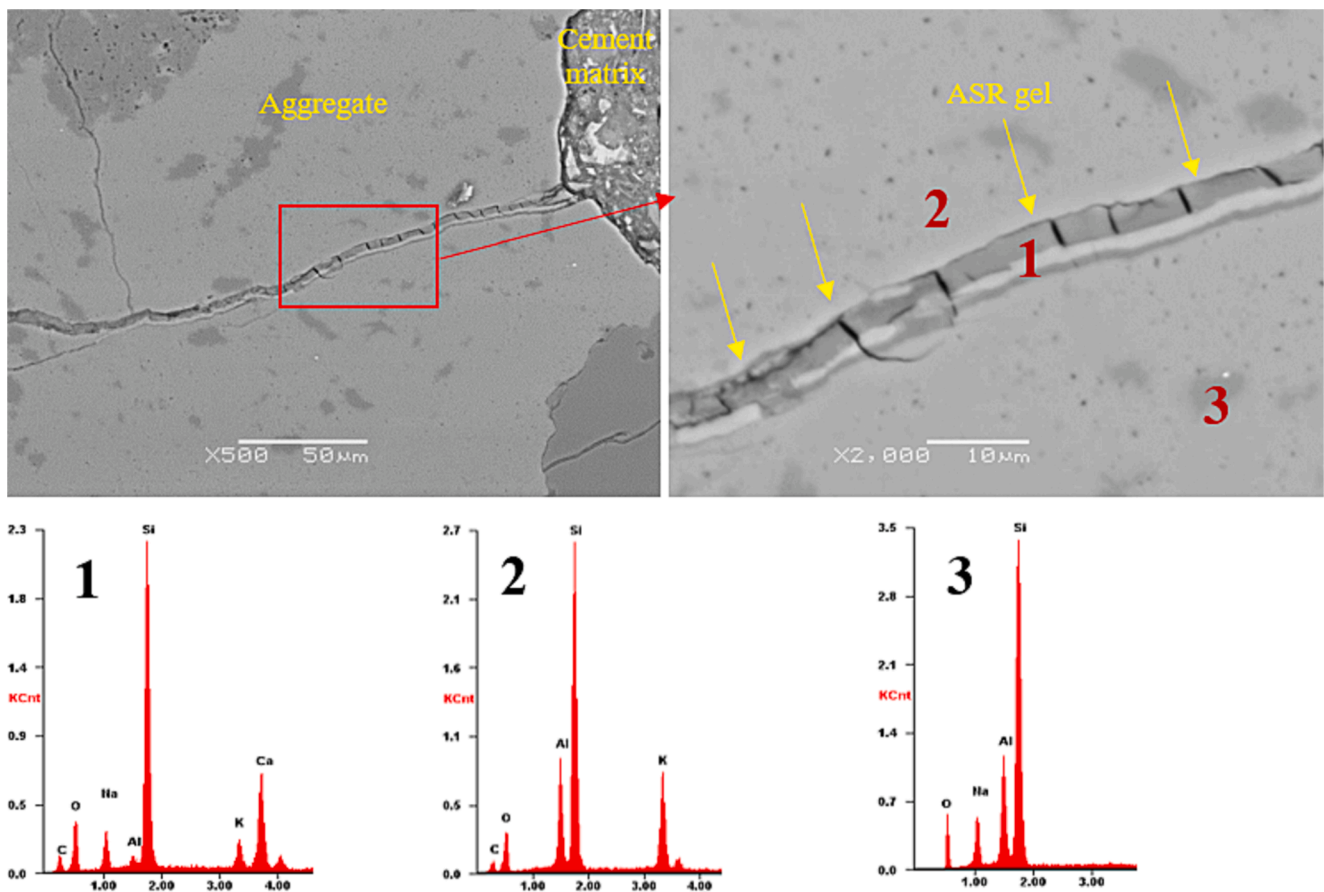
**Fig. 7.** Microphotograph of a concrete with granite aggregate (G), RILEM AAR-12 test (10% NaCl), cracked granite grain filled with ASR gel, with results of the composition analysis of marked microareas: (1) Si-Ca-Na-K gel, (2) potassium feldspar, (3) sodium feldspar.
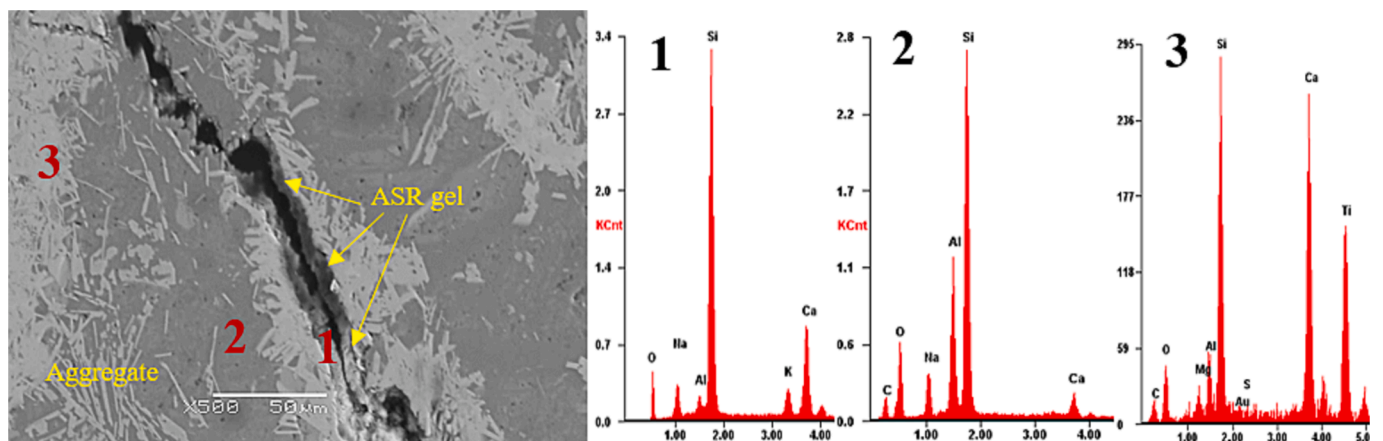


**Fig. 8.** Microphotograph of a concrete with gabbro aggregate (GA), after RILEM AAR-12 test (15% HCOONa), cracked gabbro grain filled with ASR gel, with results of the composition analysis of marked microareas: (1) Si-Ca-Na-K gel, (2) plagioclase, (3) titanite.

that increasing the alkali content in the ASR gel caused increased gel swelling and water absorption. The dependence of the expansion of concrete specimens subjected to simulated operating conditions on the alkali content in the ASR gel in aggregate cracks was found as shown in Fig. 15. A linear relationship was observed: the higher the alkali content in the ASR gel, the greater concrete expansion, with the $R^2$ determination coefficient equal to 0.86.

Both the alkali content and the type of alkali can affect the expansive properties of the gel. Leemann and Lothenbach [73] showed that higher amount of sodium than potassium in ASR products resulted in higher

expansion observed in concrete. It couldn't be confirmed with this research due to different alkali content in ASR gel depending on deicing agent type. In concrete exposed to NaCl and HCOONa in ASR gel identified in cracks in aggregate grains higher sodium content was observed, Na/K from 1.48 to 1.91 and from 1.63 to 2.03, respectively. While in concrete exposed to HCOOK in ASR gel in aggreagte cracks only potassium ions were detected (no sodium ions). Concrete in which cracks in the aggregate contained ASR gel with alkali only in the form of potassium ions showed a much greater expansion than concrete in which sodium was present in a larger amount. However, the greater expansion
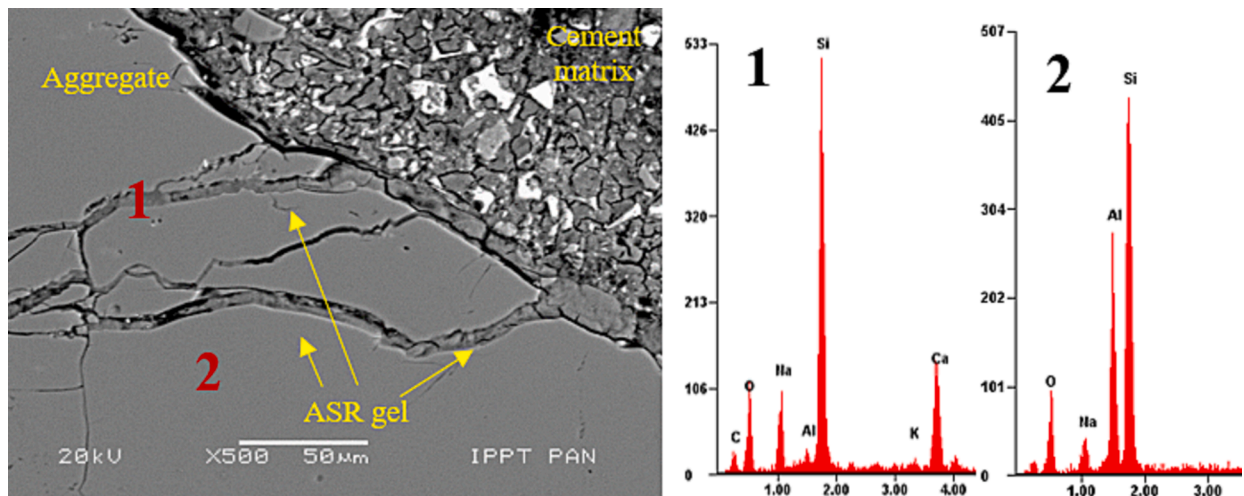
**Fig. 9.** Microphotograph of a concrete with granodiorite aggregate (GD), after RILEM AAR-12 test (15% HCOONa), cracked granodiorite grain filled with ASR gel, with results of the composition analysis of marked microareas: (1) Si-Ca-Na gel, (2) sodium feldspar.
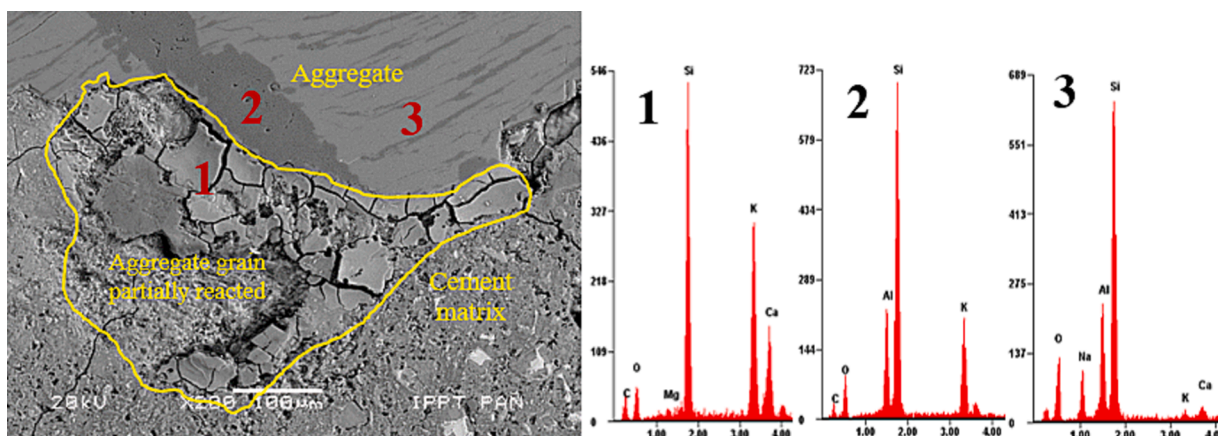


**Fig. 10.** Microphotograph of a concrete with granite aggregate (G), after RILEM AAR-12 test (50% HCOOK), granite grain partially reacted, with results of the composition analysis of marked microareas: (1) Si-Ca-K gel, (2) potassium feldspar, (3) sodium feldspar.
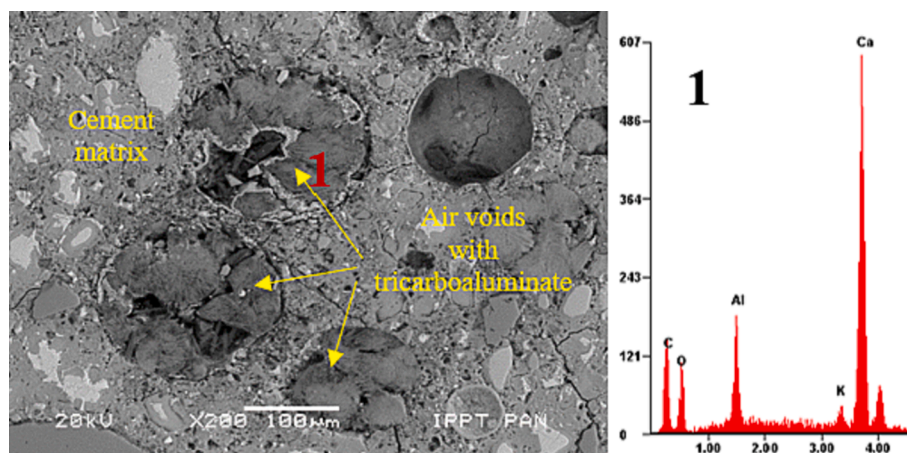


**Fig. 11.** Microphotograph of a concrete with granite aggregate (G), after RILEM AAR-12 test (50% HCOOK), air voids filled with tricarboaluminate (1).

in this case was primarily associated with a greater total alkali content rather than with their type.

## 5. Conclusions

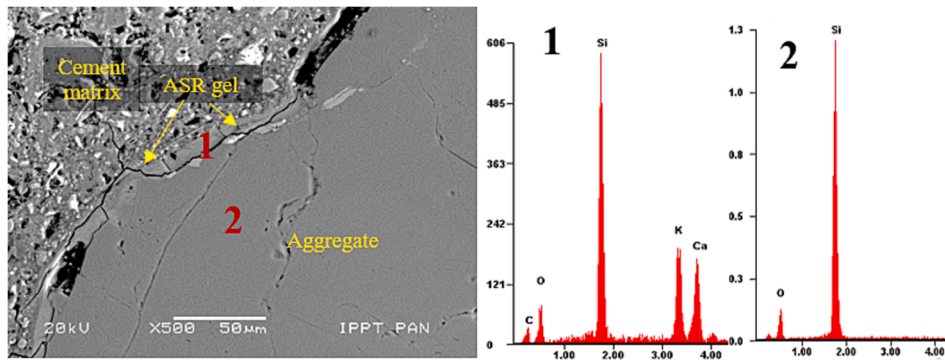Based on the conducted research, the following conclusions can be drawn:

**Fig. 12.** Microphotograph of a concrete with granodiorite aggregate (GD), after RILEM AAR-12 test (50% HCOOK), with results of the composition analysis of marked microareas: (1) Si-Ca-K gel in interfacial tranzition zone ITZ aggregate/cement matrix, (2) quartz.

**Table 7**

Chemical composition of alkali-silica reaction products localized in cracked aggregate grains in concrete after testing in simulated operating conditions (RILEM AAR-12): Ca/Si, (Na + K)/Si, Na/K (calculated on the basis of EDS atomic %).

| Aggregate | Deicing agent | Ca/Si | (Na + K)/Si | Na/K |
|---|---|---|---|---|
| G | 50% HCOOK | 0.37 ± 0.11 | 0.62 ± 0.12 | 100 % K |
| | 10% NaCl | 0.26 ± 0.12 | 0.31 ± 0.06 | 1.48 ± 0.26 |
| | 15% HCOONa | 0.36 ± 0.08 | 0.34 ± 0.05 | 1.67 ± 0.58 |
| GD | 50% HCOOK | 0.35 ± 0.07 | 0.52 ± 0.16 | 100 % K |
| | 10% NaCl | 0.29 ± 0.07 | 0.28 ± 0.09 | 1.87 ± 0.61 |
| | 50% HCOONa | 0.37 ± 0.09 | 0.36 ± 0.12 | 1.63 ± 0.32 |
| GA | 50% HCOOK | 0.45 ± 0.13 | 0.51 ± 0.13 | 100 % K |
| | 10 %NaCl | 0.30 ± 0.08 | 0.21 ± 0.07 | 1.91 ± 0.45 |
| | 15% HCOONa | 0.42 ± 0.09 | 0.35 ± 0.08 | 2.03 ± 0.53 |

- Some aggregates, despite having been previously determined as non-reactive by the standard ASR test methods, showed expansion when tested in concrete under simulated operating conditions.
- Existing methods for testing aggregates for ASR may have limitations when formate-based agents are used, therefore modified ASR test methods were used.
- The amount of concrete expansion depended on the type of an applied deicing agent.
- Deicing agents, especially sodium and potassium formate had significant influence on alkali silica reaction in concrete exposed under simulated operating conditions.
- Formates, used as an airfield deicers in quantities corresponding to field conditions, caused more severe degradation of concrete due to ASR than sodium chloride.
- Chemical composition of ASR gel in aggregate cracks was significantly affected by deicing agent type: higher content of alkali in increasing order: NaCl, HCOONa, HCOOK.
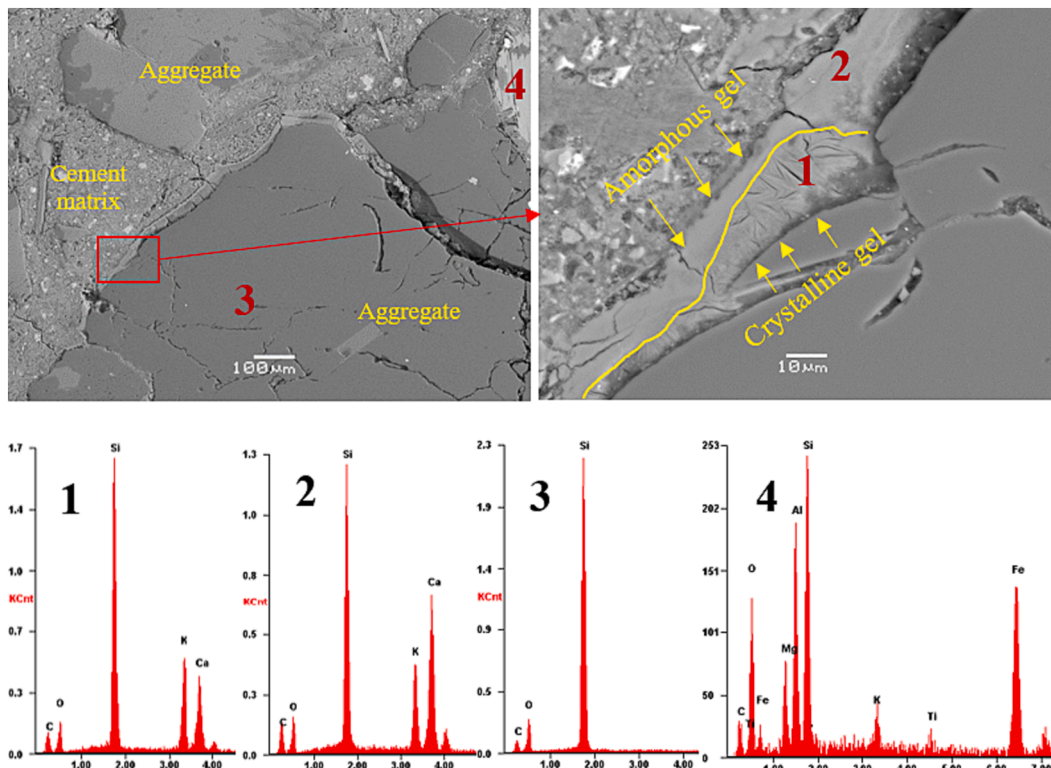


**Fig. 13.** Microphotograph of a mortar with gabbro GA aggregate, after accelerated mortar-bar test (50% HCOOK) with results of the composition analysis of marked microareas: Si-Ca-K gel in interfacial transition zone ITZ (1) crystalline, (2) amorphous, (3) quartz, (4) biotite.
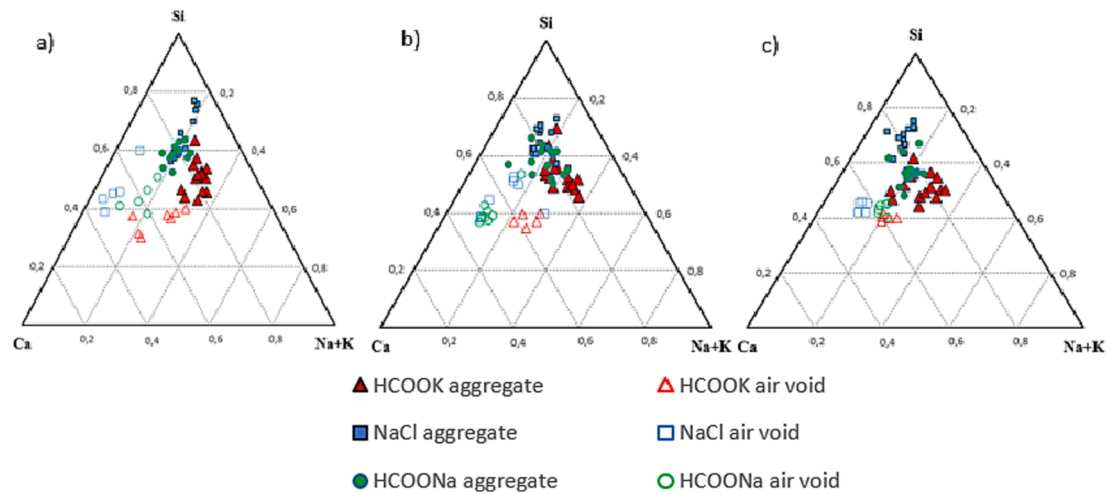
**Fig. 14.** Ternary diagram of the chemical composition of the gel located in the cracks of the aggregate grains and in the air voids in concrete-prisms with aggregate a) G, b) GD, c) GA, after testing in simulated operating conditions (RILEM AAR-12).
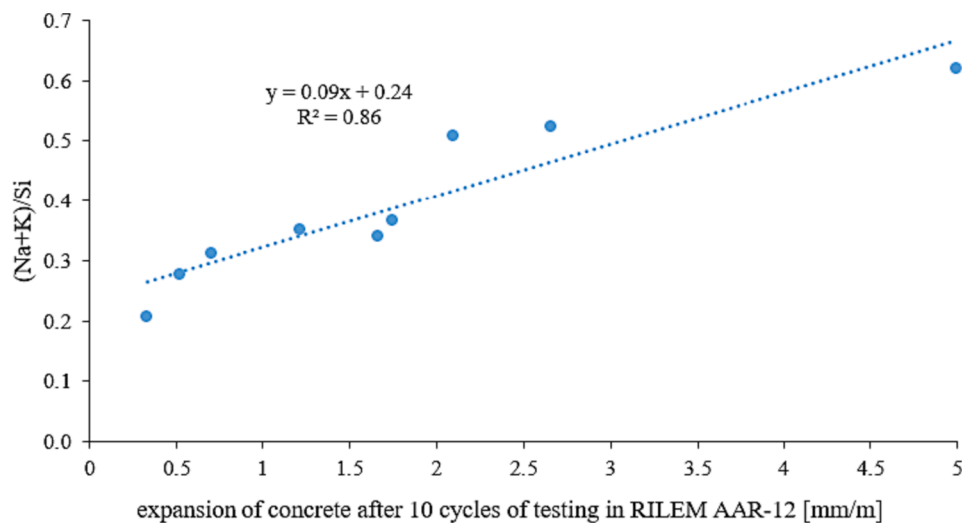


**Fig. 15.** The alkali content (Na + K)/Si in ASR gel located in cracks in aggregate grains as a function of expansion of concrete prisms after 10 cycles of testing in simulated operating conditions (RILEM AAR-12).

- Linear relationship between expansion of concrete under simulated operating conditions and alkali content in ASR gel formed in aggregate cracks was found.
- Abundance of ASR products was found in tested concrete and mortar specimens, the greatest amount of ASR gel was found in specimens exposed to 50% HCOOK solution.
- Both amorphous and crystalline ASR gels were identified, but amorphous products were dominant.

## CRediT authorship contribution statement

**A. Antolik:** Conceptualization, Formal analysis, Funding acquisition, Investigation, Methodology, Validation, Visualization, Writing – original draft, Writing – review & editing. **D. Jóźwiak-Niedźwiedzka:** Formal analysis, Methodology, Supervision, Writing – review & editing.

## Declaration of Competing Interest

The authors declare the following financial interests/personal relationships which may be considered as potential competing interests: Aneta Antolik reports financial support was provided by National

Science Centre Poland.

## Data availability

Data will be made available on request.

## References

[1] G. Plusquellec, M.R. Geiker, J. Lindgård, K. De Weerdt, Determining the free alkali metal content in concrete – Case study of an ASR-affected dam, Cem. Concr. Res. 105 (2018) 111–125, https://doi.org/10.1016/j.cemconres.2018.01.003.
[2] R.B. Figueira, R. Sousa, L. Coelho, M. Azenha, J.M. de Almeida, P.A.S. Jorge, C.J. R. Silva, Alkali-silica reaction in concrete: Mechanisms, mitigation and test methods, Constr. Build. Mater. 222 (2019) 903–931, https://doi.org/10.1016/j. conbuildmat.2019.07.230.

[3] A.K. Saha, M.N.N. Khan, P.K. Sarker, F.A. Shaikh, A. Pramanik, The ASR mechanism of reactive aggregates in concrete and its mitigation by fly ash: A critical review, Constr. Build. Mater. 171 (2018) 743–758, https://doi.org/10.1016/j.conbuildmat.2018.03.183.

[4] R. Brueckner, N. Ndugga, T.C. Meri, M.G. Alexander, H. Beushausen, F. Dehn, P. Moyo, Effects of alkali-silica reaction on a hydropower structure after 50 years of ongoing deterioration, MATEC Web Conf. 199 (2018) 03008, https://doi.org/10.1051/matecconf/201819903008.

[5] N.P. Hasparyk, P.N. Silva, D.G. Batista, H.H.A.B. Silva, H. Carasek, A.J.C. T. Cavalcanti, Assesment of alkali-silica reaction in some concretes from Brazilian hydroelectric power plants, Proc. 16th Int. Conf. Alkali-Aggregate React. Concr. (2020).

[6] E.G. Moffatt, M.D.A. Thomas, S. Hayman, B. Fournier, J. Ideker, Remediation strategies intended for the reconstruction of the ASR-induced Mactaquac dam, Proc. 15th Int. Conf. Alkali-Aggregate React. Concr. (2016).

[7] S.S. Kongshaug, M.A.N. Hendriks, T. Kanstad, G. Markeset, Toward identifying the ASR-induced stresses from displacement measurements and crack observations—Demonstration on a beam bridge in Norway, Eng. Struct. 263 (2022), 114337, https://doi.org/10.1016/j.engstruct.2022.114337.

[8] L. Kristufek, A. Zahedi, D. Tawil, L. Sanchez, B. Martin-Perez, M. Noël, H. Beushausen, J. Ndawula, M.G. Alexander, F. Dehn, P. Moyo, Preliminary evaluation of Pier cap from an ASR affected bridge in Central Canada, MATEC Web Conf. 364 (2022), 03005, https://doi.org/10.1051/matecconf/202236403005.

[9] S. Fukada, M.T. Ha, K. Torii, M. Tsuda, S. Ura, T. Sasatani, Long-term monitoring for ASR-deteriorated PC rigid-frame bridge, J. Disaster Res. 12 (3) (2017) 396–405.

[10] Š. Šachlová, R. Přikryl, Z. Pertold, Alkali-silica reaction products: Comparison between samples from concrete structures and laboratory test specimens, Mater. Charact. 61 (2010) 1379–1393, https://doi.org/10.1016/j.matchar.2010.09.010.

[11] S.A. Marfil, P.J. Maiza, Deteriorated pavements due to the alkali-silica reaction: A petrographic study of three cases in Argentina, Cem. Concr. Res. 31 (2001) 1017–1021, https://doi.org/10.1016/S0008-8846(01)00508-7.

[12] A. Antolik, D. Jóźwiak-Niedźwiedzka, Assessment of the alkali-silica reactivity potential in granitic rocks, Constr. Build. Mater. 295 (2021), 123690, https://doi.org/10.1016/j.conbuildmat.2021.123690.

[13] M.A. Glinicki, D. Jóźwiak-Niedźwiedzka, A. Antolik, K. Dziedzic, M. Dąbrowski, K. Bogusz, Diagnosis of ASR damage in highway pavement after 15 years of service in wet-freeze climate region, Case Stud. Constr. Mater. 17 (2022), e01226.

[14] P.R. Rangaraju, K.R. Sompura, J. Olek, Investigation into potential of alkali-acetate-based deicers to cause alkali-silica reaction in concrete, Transp. Res. Rec. (2006) 69–78, https://doi.org/10.3141/1979-11.

[15] C. Giebson, K. Seyfarth, J. Stark, Influence of acetate and formate-based deicers on ASR in airfield concrete pavements, Cem. Concr. Res. 40 (2010) 537–545, https://doi.org/10.1016/j.cemconres.2009.09.009.

[16] F. Rajabipour, E. Giannini, C. Dunant, J.H. Ideker, M.D.A. Thomas, Alkali – silica reaction : Current understanding of the reaction mechanisms and the knowledge gaps, Cem. Concr. Res. 76 (2015) 130–146, https://doi.org/10.1016/j.cemconres.2015.05.024.

[17] S. Hayman, M. Thomas, T. Drimalas, K. Folliard, Deterioration of concretes exposed to potassium acetate due to alkali-silica reaction. 14th Int. Conf. Alkali Aggreg. React., 2012.

[18] R. Rangaraju, P.K. Sompura, J. Desai, J. Olek, Potential of potassium acetate deicer to induce ASR in concrete, and its mitigation, Airf. Highw. Pavements. (2006) 486–497.

[19] M.A. Bérubé, J.F. Dorion, J. Duchesne, B. Fournier, D. Vézina, Laboratory and field investigations of the influence of sodium chloride on alkali – silica reactivity, Cem. Concr. Res. 33 (1) (2003) 77–84.

[20] Y. Kawabata, C. Dunant, K. Yamada, K. Scrivener, Impact of temperature on expansive behavior of concrete with a highly reactive andesite due to the alkali–silica reaction, Cem. Concr. Res. 125 (2019), 105888, https://doi.org/10.1016/j.cemconres.2019.105888.

[21] B. Fournier, J.H. Ideker, K.J. Folliard, M.D.A. Thomas, P.C. Nkinamubanzi, R. Chevrier, Effect of environmental conditions on expansion in concrete due to alkali-silica reaction (ASR), Mater. Charact. 60 (2009) 669–679, https://doi.org/10.1016/j.matchar.2008.12.018.

[22] S. Poyet, A. Sellier, B. Capra, G. Thèvenin-Foray, J.-M. Torrenti, H. Tournier-Cognon, E. Bourdarot, Influence of water on Alkali-Silica Reaction: experimental study and numerical simulations, J. Mater. Civ. Eng. 18 (4) (2006) 588–596.

[23] B.P. Gautam, D.K. Panesar, The effect of elevated conditioning temperature on the ASR expansion, cracking and properties of reactive Spratt aggregate concrete, Constr. Build. Mater. 140 (2017) 310–320, https://doi.org/10.1016/j.conbuildmat.2017.02.104.

[24] F. Weise, J. von Werder, T. Manninger, B. Maier, M. Fladt, S. Simon, A. Gardei, D. Hoehnel, S. Pirskawetz, B. Meng, A Multiscale and multimethod approach to assess and mitigate concrete damage due to alkali-silica reaction, Adv. Eng. Mater. 24 (6) (2022), 2101346, https://doi.org/10.1002/adem.202101346.

[25] T.E. Stanton, Expansion of concrete through reactionn between cement and aggregate, Proc. Am. Soc. Civ. Eng. 66 (1940) 1781–1811.

[26] I. Fernandes, M.A.T.M. Broekmans, Alkali – Silica reactions: An overview . Part I, (2013). https://doi.org/10.1007/s13632-013-0085-5.

[27] J. Jain, J. Olek, A. Janusz, D. Jóźwiak-Niedźwiedzka, Effects of deicing salt solutions on physical properties of pavement concretes, Transp. Res. Rec. 2290 (2012) 69–75, https://doi.org/10.3141/2290-09.

[28] M.A. Glinicki, R. Jaskulski, M. Dąbrowski, Design principles and testing of rinternal resistance of concrete for road structures – critical review, Roads and Bridges - Drogi i Mosty 15 (2016) 21–43, https://doi.org/10.7409/rabdim.016.002.

[29] L. Sutter, T. Van Dam, K.R. Peterson, D.P. Johnston, Long-term effects of magnesium chloride and other concentrated salt solutions on pavement and structural phase I results, Transp. Res. Recor. (2006) 60–68.

[30] K. Wang, D.E. Nelsen, W.A. Nixon, Damaging effects of deicing chemicals on concrete materials, Cem. Concr. Compos. 28 (2006) 173–188, https://doi.org/10.1016/j.cemconcomp.2005.07.006.

[31] M.C. Santagata, M. Collepardi, The effect of CMA deicers on concrete properties, Cem. Concr. Res. 30 (9) (2000) 1389–1394.

[32] F. Althoey, B. Wisner, A. Kontsos, Y. Farnam, Cementitious materials exposed to high concentration of sodium chloride solution : Formation of a deleterious chemical phase change, Constr. Build. Mater. 167 (2018) 543–552, https://doi.org/10.1016/j.conbuildmat.2018.02.066.

[33] P. Desai, Alkali Silica reaction under the influence of chloride based deicers, (2010).

[34] C.Y. Chiu, The effects of chloride-based deicing chemicals on degradation of portland cement mortars with alkali reactive aggregate, Open Access Dissertations (2016).

[35] X. Shi, L. Fay, M.M. Peterson, M. Berry, M. Mooney, A FESEM / EDX investigation into how continuous deicer exposure affects the chemistry of Portland cement concrete, Constr. Build. Mater. 25 (2011) 957–966, https://doi.org/10.1016/j.conbuildmat.2010.06.086.

[36] M. Kawamura, M. Ichise, Characteristics of alkali-silica reaction in the presence of sodium and calcium chloride, Cem. Concr. Res. 20 (1990) 757–766, https://doi.org/10.1016/0008-8846(90)90009-M.

[37] M.-A. Bérubé, J. Frenette, Testing concrete for AAR in NaOH and NaCl solutions at 38 ° C and 80 ° C, Cem. Concr. Compos. 16 (3) (1994) 189–198.

[38] G.A. Julio-Betancourt, Effect of de-icer and anti-icer chemicals on the durability, microstructure and properties of cement-based materials, (2009).

[39] P.R. Rangaraju, J. Desai, Effectiveness of fly ash andslag in mitigating alkali-silica reaction induced by deicingchemicals, J. Mater. Civ. Eng. 21 (1) (2009) 19–31.

[40] T. Iskhakov, C. Giebson, J.J. Timothy, H.M. Ludwig, G. Meschke, Deterioration of concrete due to ASR: Experiments and multiscale modeling, Cem. Concr. Res. 149 (2021), 106575, https://doi.org/10.1016/j.cemconres.2021.106575.

[41] C. Giebson, K. Seyfarth, H.-M. Ludwig, Influence of sodium chloride on ASR in highway pavement concrete, in: 15th Int. Conf. Alkali-Aggregate React. Concr., 2016, p. 10.

[42] S. Chatterji, A.D. Jensen, N. Thaulow, P. Christensen, Studies of alkali-silica reaction. Part 3. Mechanisms by which NaCl and Ca(OH)2 affect the reaction, Cem. Concr. Res. 16 (1986) 246–254, https://doi.org/10.1016/0008-8846(86)90141-9.

[43] S. Farooq, H. Yokota, Residual mechanical properties of steel fiber reinforced concrete damaged by alkali silica reaction and subsequent sodium chloride exposure, Ceram. Int. 48 (2022) 4850–24858, https://doi.org/10.1016/j.ceramint.2022.05.138.

[44] J. Chris, M.D. Affolter, I. Paul, M. Cam, An Introduction to Geology, 2023. https://doi.org/10.2307/2420180.

[45] D. Jóźwiak-Niedźwiedzka, A. Antolik, K. Dziedzic, M.A. Glinicki, K. Gibas, Resistance of selected aggregates from igneous rocks to alkali-silica reaction: verification, Roads and Bridges - Drogi i Mosty 18 (2019) 67–83, https://doi.org/10.7409/rabdim.019.005.

[46] P.J. Nixon, I. Sims, RILEM Recommendations for the Prevention of Damage by Alkali- Aggregate Reactions in New Concrete Structures. State-of-the-Art Report of the RILEM Technical Committee 219-ACS, Springer, 2016.

[47] V. Ramos, I. Fernandes, A. Santos Silva, D. Soares, B. Fournier, S. Leal, F. Noronha, Assessment of the potential reactivity of granitic rocks - Petrography and expansion tests, Cem. Concr. Res. 86 (2016) 63–77, https://doi.org/10.1016/j.cemconres.2016.05.001.

[48] I. Fernandes, F. Noronha, M. Teles, Microscopic analysis of alkali-aggregate reaction products in a 50-year-old concrete, Mater. Charact. 53 (2004) 295–306, https://doi.org/10.1016/j.matchar.2004.08.005.

[49] A. Shayan, Alkali reactivity of deformed granitic rocks: a case study, Cem. Concr. Res. 23 (5) (1993) 1229–1236.

[50] Š. Šachlová, Microstructure parameters affecting alkali-silica reactivity of aggregates, Constr. Build. Mater. 49 (2013) 604–610, https://doi.org/10.1016/j.conbuildmat.2013.08.087.

[51] D. Lu, X. Zhou, Z. Xu, X. Lan, M. Tang, B. Fournier, Evaluation of laboratory test method for determining the potential alkali contribution from aggregate and the ASR safety of the Three-Gorges dam concrete, Cem. Concr. Res. 36 (2006) 1157–1165, https://doi.org/10.1016/j.cemconres.2006.01.004.

[52] NO-17-A204 Nawierzchnie lotniskowe - Nawierzchnie z betonu cementowego - Wymagania i metody badań, (2015).

[53] PN-EN 12620+A1:2013, Aggregates for concrete.

[54] A. Garbacik, M.A. Glinicki, D. Jóźwiak-Niedźwiedzka, G. Adamski, K. Gibas, Technical Guidelines for the Classification of Domestic Aggregates and Prevention of The Alkali-Aggregate Reaction in Concrete Used in Road Pavements and Road Engineering Facilities, Institute of Ceramics and Building Materials, Institute of Fundamental Technological research of Polish Academy of Sciences, 2019.

[55] RILEM Recommended Test Method: AAR-2—Detection of Potential Alkali-Reactivity— Accelerated Mortar-Bar Test Method for Aggregates, in RILEM Recommendations for the Prevention of Damage by Alkali-Aggregate Reactions in New Concrete Structures, Eds. P.J. Nixon, I. Sims, Springer (2016).

[56] NO-17-A205 Zimowe utrzymanie naiwerzchni lotniskowych. Stosowanie środków odladzających. Wymagania i badania, (2017).

[57] RILEM Recommended Test Method: AAR-3—Detection of Potential Alkali-Reactivity—38 °C Test Method for Aggregate Combinations Using Concrete Prisms, in RILEM Recommendations for the Prevention of Damage by Alkali-Aggregate Reactions in New Concrete Structure, Eds. P.J. Nixon, I. Sims, Springer (2016).

[58] I. Borchers, Recommendation of RILEM TC 258-AAA: RILEM AAR-12: determination of binder combinations for non-reactive mix design or the resistance to alkali-silica reaction of concrete mixes using concrete prisms − 60 °C test method with alkali supply, Mater. Struct. Constr. 54 (2021), https://doi.org/10.1617/s11527-021-01681-2.

[59] PN-EN 12390-3:2011 Testing hardened concrete – Part 3: Compressive strength of test specimens.

[60] S. Chatterji, Chemistry of alkali-silica reaction and testing of aggregates, Cem. Concr. Compos. 27 (2005) 788–795, https://doi.org/10.1016/j.cemconcomp.2005.03.005.

[61] TP B-StB - Technische Prüfvorschriften für Verkehrsflächenbefestigungen – Betonbauweisen: Teil 1.1.09 AKR-Potenzial und Dauerhaftigkeit von Beton (60 -Betonversuch mit Alkalizufuhr). Ausgabe (2018).

[62] S. Math, D. Wingard, P.R. Rangaraju, Assessing potential reactivity of aggregates in presence of potassium acetate deicer: Revised mortar bar test method, Transp. Res. Rec. 2232 (1) (2011) 10–24.

[63] C.S. Rangel, M. Amario, M. Pepe, E. Martinelli, R.D.T. Filho, Influence of wetting and drying cycles on physical and mechanical behavior of recycled aggregate concrete, Materials (Basel) 13 (2020) 1–20, https://doi.org/10.3390/ma13245675.

[64] H. Ye, N. Jin, X. Jin, C. Fu, Model of chloride penetration into cracked concrete subject to drying-wetting cycles, Constr. Build. Mater. 36 (2012) 259–269, https://doi.org/10.1016/j.conbuildmat.2012.05.027.

[65] Z. Wu, H.S. Wong, N.R. Buenfeld, Transport properties of concrete after drying-wetting regimes to elucidate the effects of moisture content, hysteresis and microcracking, Cem. Concr. Res. 98 (2017) 136–154, https://doi.org/10.1016/j.cemconres.2017.04.006.

[66] C. Rößler, B. Möser, C. Giebson, H.M. Ludwig, Application of Electron Backscatter Diffraction to evaluate the ASR risk of concrete aggregates, Cem. Concr. Res. 95 (2017) 47–55, https://doi.org/10.1016/j.cemconres.2017.02.015.

[67] A. Antolik, Influence of sodium and potassium formate on the ASR reactivity of granite aggregate, Struct. Environ. 14 (2022) 69–75, https://doi.org/10.30540/sae-2022-008.

[68] A. Leemann, Z. Shi, J. Lindgård, Characterization of amorphous and crystalline ASR products formed in concrete aggregates, Cem. Concr. Res. 137 (2020), 106190, https://doi.org/10.1016/j.cemconres.2020.106190.

[69] C.M. Strack, E. Barnes, M.A. Ramsey, R.K. Williams, K.L. Klaus, R.D. Moser, Impact of aggregate mineralogy and exposure solution on alkali-silica reaction product composition and structure within accelerated test conditions, Constr. Build. Mater. 240 (2020) 117929, https://doi.org/10.1016/j.conbuildmat.2019.117929.

[70] A. Leemann, Alkali-silica reaction - sequence, products and possible mechanisms of expansion, Proc. 16th Int. Conf. Alkali-Aggregate React. Concr. Lisbon, Part. 2 (2022).

[71] A. Gholizadeh-Vayghan, F. Rajabipour, The influence of alkali–silica reaction (ASR) gel composition on its hydrophilic properties and free swelling in contact with water vapor, Cem. Concr. Res. 94 (2017) 49–58, https://doi.org/10.1016/j.cemconres.2017.01.006.

[72] A. Leemann, G. Le Saout, F. Winnefeld, D. Rentsch, B. Lothenbach, Alkali-Silica reaction: The Influence of calcium on silica dissolution and the formation of reaction products, J. Am. Ceram. Soc. 94 (2011) 1243–1249, https://doi.org/10.1111/j.1551-2916.2010.04202.x.

[73] A. Leemann, B. Lothenbach, The influence of potassium-sodium ratio in cement on concrete expansion due to alkali-aggregate reaction, Cem. Concr. Res. 38 (2008) 1162–1168, https://doi.org/10.1016/j.cemconres.2008.05.004.